Model interatomic potential for simulations in selenium

C. Oligschleger,* R. O. Jones, S. M. Reimann,† and H. R. Schober
Institut für Festkörperforschung, Forschungszentrum Jülich, D-52425 Jülich, Germany
(Received 6 October 1995)

A three-body, effective interatomic potential is described for selenium. The form is similar to that used for sulfur by Stillinger and Weber, and the parameters are determined using the structures and energies of Se clusters (Se_2-Se_8), known from experiment and density functional calculations, and refined using data for various crystal phases. The potential reproduces the main structural and dynamical features of Se molecules and crystals, and we give results for structures, binding energies, vibrations, and elastic constants of different Se phases.

I. INTRODUCTION

The description and prediction of properties of real molecules and condensed systems is of great importance in physics, chemistry, and technology. Many phenomena involve large numbers of atoms and long time scales, so that a simplified description of the energy and the forces in the system, and their dependence on structure, is often unavoidable. In such cases, it is common to apply Born–von Kármán like models, where the energy is expanded quadratically around appropriate bond lengths and angles. This is a standard method for parametrizing phonon dispersion curves of crystals of metals and covalent materials,[1] but its application to disordered structures is limited by the quadratic approximation. In particular, changes in the local topology (bond breaking and variations in the coordination number) cannot be treated adequately. Nevertheless, with suitable assumptions about the basic building blocks these methods can be employed successfully.[2]

A microscopic approach to the problem of determining forces and energies in a system is provided by the density functional (DF) formalism.[3] With relatively simple approximations for the density dependence of the exchange-correlation energy, this scheme allows one to calculate cohesive and structural properties without using adjustable parameters, although the widely used local spin density (LSD) approximation often leads to an overestimate of the binding energies.[3] The combination of DF calculations with molecular dynamics (MD) (Ref. 4) provides a scheme that does not depend on assumptions about the geometry of the system, and has been used to predict the structures of many molecules and to provide MD simulations on liquids and amorphous materials. However, the complexity of the calculations—which arises from the requirement to treat the electronic degrees of freedom—presently limits applications to systems with ~ 100 atoms and to time scales of the order of picoseconds.[5] These restrictions currently rule out the study of many interesting properties.

We address here an alternative approach to these problems, the description of interatomic interactions by effective potentials that can be adjusted to describe known properties of, for example, molecules, crystals, and crystal defects. This approach does not treat explicitly the electronic degrees of freedom and favors a convenient description of the forces and energies in a range of environments over the exact description of a single structure. We present here a model three-body potential designed to reproduce geometries and energies in both molecular and crystalline phases of selenium.

Selenium readily forms glasses and amorphous structures, and the industrial relevance of many of their properties—such as photodarkening—have made it the subject of many studies over the past decades. These include MD/DF simulations on the liquid and amorphous phases,[5] and studies of the chain structure in liquid Se using MD studies with parametrized force fields[2] and tight-binding Monte Carlo methods.[6] There are several crystalline structures, including two (α- and β-) monoclinic forms with four eight-membered rings packed differently in the unit cell. The most stable crystalline phase under normal pressures consists of infinite helical chains with trigonal symmetry.[7,8]

The crystallographic information could be used to parametrize force laws, but Se has a particular advantage that it belongs to the sixth main group and, like its neighbor sulfur, forms many stable, ringlike structures with twofold coordination. Mass spectroscopy of Se vapor shows the existence of clusters with up to 40 atoms,[9,10] and the structures of Se_2-Se_8 have either been measured or predicted by MD/DF calculations.[11] The calculations give very good agreement with experimental structures in cases where spectroscopic data are available, so that the predictions of unknown structures should be reliable. Subsequent vacuum UV photoelectron spectra of Se_5-Se_8,[10] for example, were consistent with the MD/DF predictions of the structures for Se_5 and Se_7. These structural data, and the related binding energies, can be used to model an effective potential for use in simulations of, e.g., the amorphous structures of Se. We describe the covalent bonding between Se atoms using short-range interactions, and we neglect the weaker long-range Coulomb contributions for simplicity.

In Sec. II we describe how the potential parameters are determined from the structures and binding energies of small Se clusters, and refined using properties of the trigonal and α-monoclinic allotropes of Se, including geometries, energies, and phonon frequency spectra.[7,8] We discuss the form of the potential. In Sec. III we give results for molecules and crystals and compare them with MD/DF calculations and experiment. We summarize our findings in Sec. IV. Structural changes occurring during the glass transition and the local-

0163-1829/96/53(10)/6165(9)/$10.00

ized vibrations and relaxations in Se glasses have been discussed elsewhere.[12,13]

II. POTENTIAL

Short-ranged pair potentials cannot be used to model covalently bonded systems, and we have adopted a three-body potential of the form used by Stillinger and Weber[14] for simulations in sulfur. In the case of selenium, our first step is to fit the potential parameters to the structures and energies of small clusters. We then assess how well this potential describes bulk properties and make modifications necessary to provide a reasonable description of both clusters and bulk.

The structural information used as input for the fitting procedure comes from Se_2, the Se_3 trimer in both its triangular (D_{3h}) and open (C_{2v}) forms, Se_4, Se_5, Se_6 in its boat (C_{2v}) structure, and the crown-shaped structure (D_{4d}) of Se_8. As we have noted above, the structures calculated by the MD/DF method[11] should be very reliable, with uncertainties in the bond lengths of ~ 0.05 Å and bond angles of $\sim 1°$. The MD/DF calculations use the LSD approximation to the exchange-correlation energy. While the energy differences between different isomers of the same cluster should be accurate to ~ 5 meV/atom (structures with energy differences within this range will be viewed as degenerate), the binding or formation energies are overestimated, and we use instead the binding energies determined in measurements on Se vapor.[15] Using a least-squares fit procedure,[16] we adjust the parameters of the model potential to reproduce the above structures (determined from the necessary condition that the forces on the nuclei vanish) and to have binding energies within 5 meV/atom of the experimental values. Since optimization usually results in a local minimum in the space of the adjustable parameters, the procedure has been repeated with a range of starting values.

Application of the model potential so obtained to the trigonal crystal phase results at $T=0$ K in a shift and rotation of the Se chains relative to each other. This is not unexpected, since the database for the fitting procedure uses data from small clusters of finite extent, and the three-dimensional structure also involves the longer-range interaction between the chains. In a second step we have modified the potential to reproduce the above structures for Se_2-Se_8[11] *and* those of the trigonal and orthorhombic crystalline phases, which comprise parallel chains and eight-membered rings, respectively. Stabilization of the trigonal phase required a change in the range of the potential, which was adjusted so that this structure was more stable than the amorphous and the two monoclinic forms.

Our final effective interatomic potential U is strongly repulsive for small interatomic distances and includes two- and three-particle interactions [we use "reduced" units (r.u.) based on the experimental bond length (1.337 r.u. = 2.34 Å) and dissociation energy (0.697 r.u. = 2.24 eV) of the Se_8 molecule]:

$$U=\sum_{i<j} V_2(r_{ij})+\sum_{i<j<k} h(r_{ij},r_{kj},\Theta_{ijk}) + \text{cyclic permutations}, \quad (1)$$

where $V_2(r_{ij})$ is the two-particle contribution of the potential energy U for atoms i and j separated by distance r_{ij}. The three-body interaction depends on r_{ij}, r_{jk}, and Θ_{ijk}, the angle at atom j subtended by r_{ij} and r_{jk}. The three-particle energy $h(r,s,\theta)$ is given by

$$h(r,s,\theta)=V_3(r)V_3(s)[b_1(\cos\theta-\cos\beta_2)^2 + b_3-0.5b_1\cos^4\theta], \quad (2)$$

with $b_1=34.4866$, $b_3=11.9572$, and $\beta_2=95.3688°$. The three-body term is purely repulsive and strongly favors a coordination number of two as observed in experiment. The angular dependence reflects the preference for θ values of $\approx 100°$. The $\cos^4$ term is a slight modification introduced to stabilize the Se chains of the trigonal phase against torsion relative to each other.

To simplify numerical calculations we describe the radial parts of the two- and three-body potential of Eqs. (1) and (2) by decaying exponential functions. Discontinuities in the vibration frequencies are avoided by cutting off the potentials smoothly by polynomials to yield continuous functions with continuous first and second derivatives at the cutoff distances:

$$V_{2,3}(r)=a_{2,3}\exp(\alpha r)+b_{2,3}\exp(\beta r) + c_{2,3}\exp(\gamma r), \quad r<1.6 \quad (3)$$

$$=d_{2,3}(r-r_{2,3})^5+e_{2,3}(r-r_{2,3})^4 + f_{2,3}(r-r_{2,3})^3, \quad 1.6<r<r_{2,3} \quad (4)$$

$$=0, \quad r>r_{2,3}.$$

The exponential part of the interaction potential takes the nearest-neighbor shell into account (1.6 r.u.=2.79 Å), while the long-range behavior is described by the cutoff function. The cutoff distances are denoted by $r_{2,3}$ for the two- and three-body potentials, respectively. The radial parts of these potentials are shown in Fig. 1, and the corresponding parameters are listed in Table I. Using this set of parameters we can describe both molecules and crystalline phases.

III. RESULTS

The above potential was designed to reproduce the gross features of Se molecules and crystals. A number of compromises have been necessary, so that the quality of the potential should be assessed by its overall description of many different quantities. We now report the properties calculated with our model for a number of molecules and crystalline modifications. For the former we determine ground-state energies, structures (bond lengths and angles), and vibrational frequencies, for the crystals we also give vibrational frequencies and elastic constants calculated at $T=0$ K in the harmonic approximation. The potential can easily be modified, of course, if it is required to reproduce some particular property more accurately.

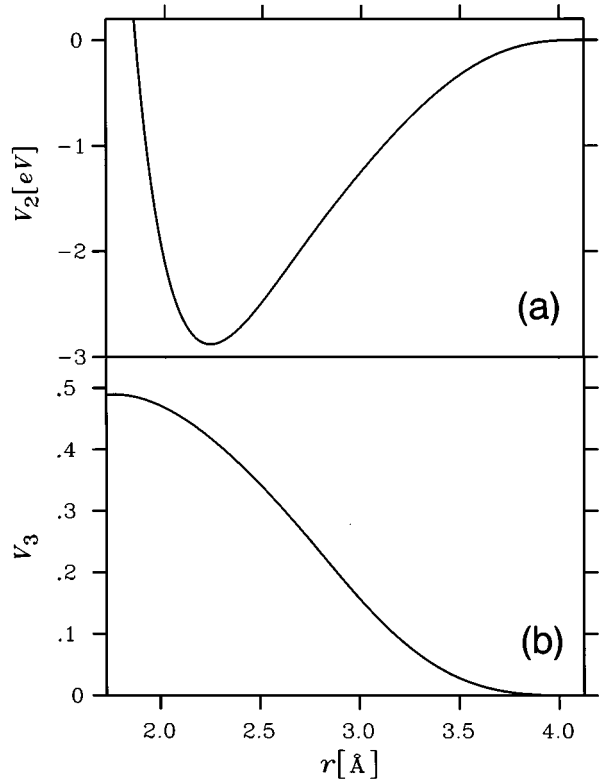

FIG. 1. (a) Two-body potential V_2, and (b) three-body potential V_3 as a function of interatomic separation r (Å).

A. Molecules

The group VIa elements sulfur,[17] selenium, and tellurium[9] show a variety of clusters in the gas phase. Mass spectroscopy measurements on selenium show stable molecules with up to 40 atoms,[9,10] and cluster binding energies have been deduced from gas phase experiments.[15] In this subsection we report the structures and energies of small Se clusters obtained with our parametrized potential and compare them with experiments and DF results where possible. In Table II we summarize the results for bond lengths and bond angles in Se_2-Se_8, and in Table III the results for the binding en-

TABLE I. Parameters for the two- and three-body potential (in r.u.).

	Two-body potential $r<1.6$	Three-body potential $r<1.6$
a	928.12	8.8297
b	0.26802	−2.5932
c	−16.599	−6.9384
α	−7.984	−0.47601
β	−0.000077781	−1.5637
γ	−1.8634	−0.37049
	$1.6<r<2.37$	$1.6<r<2.35$
d	1.86825	0.22556
e	4.58628	0.12527
f	3.62029	−0.21019
$r_{2,3}$	2.37	2.35

TABLE II. Structure parameters for small Se molecules from present work, MD/DF calculations (Ref. 11), and experiment. Bond lengths d_{ij} in Å, bond angles α_i and dihedral angles γ_{ij} (at bond ij) in degrees, frequencies ν in THz.

n		this work	MD/DF	experiment
2	d	2.23	2.20	2.17
	ν	9.66	11.0	11.55
3 D_{3h}	d	2.36	2.37	-
	α	60°	60°	-
	ν_1	5.08	-	-
	ν_2	8.20	-	-
3 C_{2v}	d	2.26	2.20	-
	α	94.4°	118°	115°
	ν_1	3.05	-	-
	ν_2	8.75	-	-
	ν_3	8.98	-	9.36
4 C_{2v}	$d_{12,34}$	2.40	2.17	-
	d_{23}	2.40	2.42	-
	α	90°	108°	-
4 C_{2h}	$d_{12,34}$	2.28	2.20	-
	d_{23}	2.33	2.40	-
	α	99.2°	110°	-
5 C_s	d	2.32-2.34	2.29-2.46	-
	α_1	71.4°	87°	-
	α_{2-5}	99.3°	100°	-
6 D_{3d}	d	2.33	2.35	2.34
	α	99.4°	101°	101.3°
	γ	78.7°	76°	76.2°
6 C_{2v}	$d_{12,16,34,45}$	2.33	2.31	-
	$d_{23,56}$	2.33	2.52	-
	$\alpha_{2,3,5,6}$	102°	107°	-
	$\alpha_{1,4}$	99°	98°	-
	γ	75.8°	79°	-
7 C_s "chair"	$d_{12,17}$	2.34	2.36	-
	$d_{23,67}$	2.34	2.42	-
	$d_{34,56}$	2.34	2.27	-
	d_{45}	2.34	2.50	-
	$\alpha_{1,3,6}$	100°	106°	-
	$\alpha_{2,7}$	99°	101°	-
	$\alpha_{4,5}$	101°	105°	-
	$\gamma_{12,71}$	71°	75°	-
	$\gamma_{23,67}$	117°	110°	-
	$\gamma_{34,56}$	92°	86°	-
7 C_s "boat"	$d_{12,17}$	2.34	2.32	-
	$d_{23,67}$	2.34	2.46	-
	$d_{34,56}$	2.34	2.23	-
	d_{45}	2.34	2.55	-
	α_1	98°	108°	-
	$\alpha_{2,7}$	100°	100°	-
	$\alpha_{3,6}$	99°	108°	-
	$\alpha_{4,5}$	101°	108°	-
	$\gamma_{12,71}$	72°	71°	-
	$\gamma_{23,67}$	41°	44°	-
	$\gamma_{34,56}$	92°	89°	-
8 D_{4d}	d	2.33	2.34	2.34
	α	100°	105°	105.7°
	γ	107°	101°	101.3°
	ν	0.8−7.9		1.4−7.7

TABLE III. Binding energies E (eV/atom) of Se molecules from present work, MD/DF calculations (Ref. 11), and experiment (Ref. 15).

n	This work	MD/DF	Experiment
2	1.44	2.28	1.54−1.72
3 D_{3h}	1.67	2.77	-
3 C_{2v}	1.74	2.77	1.82
4 C_{2v}	2.07	2.95	1.95
4 C_{2h}	1.84	2.88	1.95
5 C_s	2.20	3.17	2.14
6 D_{3d}	2.24	3.22	2.19
6 C_{2v}	2.24	3.16	-
7 C_s "chair"	2.26	3.25	2.21
7 C_s "boat"	2.27	3.24	2.21
8 D_{4d}	2.24	3.28	2.24

ergies. The structures of Se_3, Se_4, and Se_5 are given in Fig. 2 and those of Se_6, Se_7, and Se_8 in Fig. 3.

1. Se_2

For the dimer we calculate a bond length of 2.23 Å and a binding energy of 1.44 eV/atom. The experimental bond length is 2.17 Å and the estimated binding energies range from 1.54–1.72 eV/atom.[18,19] The calculated vibration frequency (9.66 THz) is lower than the experimental value (11.55 THz).[20]

2. Se_3

The model potential gives two nearly degenerate structures, a triangular structure (D_{3h}) and an open form (C_{2v}).

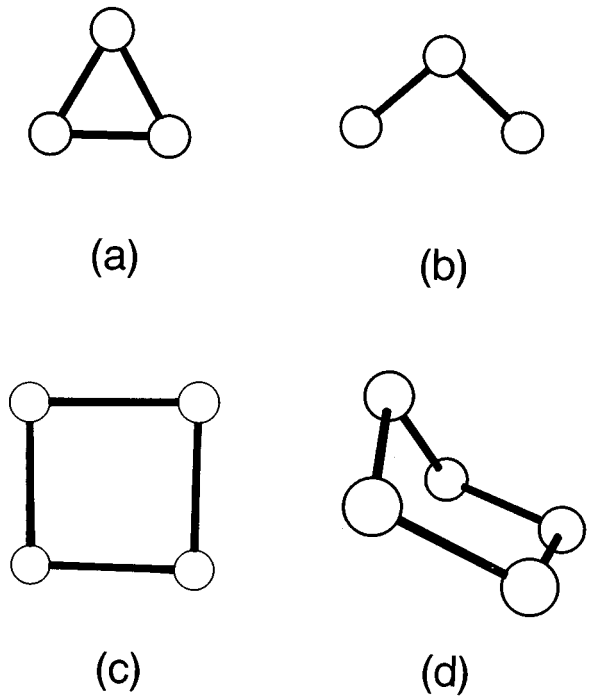

FIG. 2. (a) and (b) Structures of Se_3, (c) Se_4 (D_{4h}), (d) Se_5 (C_s).

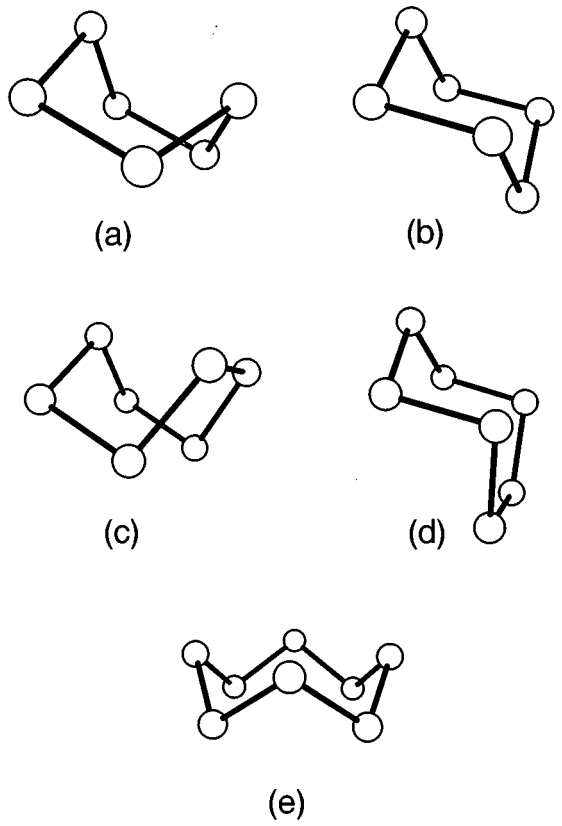

FIG. 3. (a) Boat and (b) chair structures of Se_6, (c) boat and (d) chair structures of Se_7, (e) Se_8 (D_{4d}).

The former (d=2.36 Å, α=60°) agrees well with that of Ref. 11 and has a binding energy of 1.67 eV/atom. For symmetry reasons there are only two different vibrational frequencies, ν_1=5.08 and 8.20 THz. For the open structure we obtain d=2.26 Å, α=94.4°, and a binding energy of 1.74 eV/atom. The vibrational frequencies are 3.05, 8.75, and 8.98 THz.

The MD/DF calculations give a bond length d=2.20 Å for the open structure, with α=118°. Resonance Raman spectroscopy of matrix isolated Se_3 (Ref. 21) appears to rule out the existence of a triangular structure, and Schnöckel, Göcke, and Elsper[21] associate the measured bands with an open structure with bond angle $\alpha\sim$115°. The experimental bond stretching frequency is 9.32 THz, and the binding energy (1.82 eV/atom) (Ref. 15) is slightly higher than our value.

3. Se_4

There is little experimental information on the structures of Se_4, although the binding energy (1.95 eV/atom) has been determined from gas phase experiments.[15] MD/DF calculations lead to a planar, trapeze-shaped (C_{2v}) ground state, with binding energy 2.95 eV/atom, bond lengths $d_{12,34}$=2.17 Å, and d_{23}=2.42 Å, and bond angles $\alpha_{2,3}$= 108°. There is a similar pattern of bond lengths in a C_{2h} configuration (binding energy 2.88 eV/atom, $d_{12,34}$=2.20 Å, d_{23}=2.40 Å, and bond angles $\alpha_{2,3}$=110°).

Our model potential leads to a ground state that is square (D_{4h}), with bond length d=2.4 Å and binding energy E of

2.07 eV/atom. A chainlike (C_{2h}) structure is also stable, with $E=1.84$ eV/atom, bond lengths $d_{12,34}=2.28$ Å, $d_{23}=2.33$ Å, and bond angles $\alpha_{2,3}=99.2°$.

4. Se_5

The model potential leads to a stable structure with the "envelope" (C_s) structure. The bond lengths lie between $d=2.32$–2.34 Å, and the bond angles are $\alpha_1=71.4°$ and $\alpha_{2-5}=99.3°$. The binding energy is 2.20 eV/atom, compared with the measured value of 2.14 eV/atom.[15] The MD/DF calculations also lead to a ground state with C_s structure, but with a binding energy of 3.17 eV/atom. The bond lengths lie between 2.29–2.46 Å, and the bond angles are $\alpha_1=87°$ and $\alpha_{2-5}=100°$.

5. Se_6

A crystalline phase comprising Se_6 molecules with D_{3d} symmetry is well known.[7] The structure parameters are $d=2.34\pm0.01$ Å, $\alpha=101.3\pm0.3°$, and $\gamma=76.2\pm0.4°$, and the binding energy in the gas phase is 2.19 eV/atom. The most stable isomer of Se_6 found using our model potential also has D_{3d} symmetry. The bond length (2.33 Å), bond angle (99.4°), and dihedral angle (78.7°) agree well with the measured values. The calculated binding energy is 0.05 eV/atom higher than the experimental value.

A second stable Se_6 structure with C_{2v} symmetry has bond length 2.33 Å, bond angles $\alpha_{2,3,5,6}=102°$ and $\alpha_{1,4}=99°$, and dihedral angle 75.8°. MD/DF calculations give for this structure $d_{12,16,34,45}=2.31$ Å and two longer bonds with $d_{23,56}=2.52$ Å, bond angles $\alpha_{2,3,5,6}=107°$, $\alpha_{1,4}=98°$, and dihedral angle 79°. The two long bonds of the C_{2v} molecule are not reproduced by our model potential. This structure has not yet been observed.

6. Se_7

MD/DF calculations give two structures with C_s symmetry: The more stable ("chair") form has bond lengths $d_{12,17}=2.33$ Å, $d_{23,67}=2.41$ Å, $d_{34,56}=2.26$ Å, and $d_{45}=2.49$ Å, bond angles $\alpha_{1,3,6}=106°$, $\alpha_{2,7}=101°$, and $\alpha_{4,5}=105°$, and dihedral angles $\gamma_{12,71}=75°$, $\gamma_{23,67}=110°$, and $\gamma_{34,56}=86°$. The binding energy is 3.25 eV/atom. A second minimum has the "boat" structure and bond lengths $d_{12,17}=2.32$ Å, $d_{23,67}=2.46$ Å, $d_{34,56}=2.23$ Å, and $d_{45}=2.55$ Å, bond angles $\alpha_{1,3,6}=108°$, $\alpha_{2,7}=100°$, and $\alpha_{4,5}=108°$, and dihedral angles $\gamma_{12,71}=71°$, $\gamma_{23,67}=44°$, and $\gamma_{34,56}=89°$. The calculated binding energy is 3.24 eV/atom, significantly higher than the gas phase estimate (2.21 eV/atom).

The model potential also yields a "boat" isomer with C_s symmetry. In contrast to the DF calculation, however, the bond length is constant (2.34 Å) and not alternating. The calculated energy is only 0.05 eV/atom higher than the experimental value. We find an additional minimum with a "chair" structure and binding energy 2.27 eV/atom. All bonds have length 2.34 Å, and the bond angles are $\alpha_{1,3,6}=100°$, $\alpha_{2,7}=99°$, and $\alpha_{4,5}=101°$, and dihedral angles $\gamma_{12,71}=71°$, $\gamma_{23,67}=117°$, and $\gamma_{34,56}=92°$.

7. Se_8

The Se_8 molecule with a crown-shaped (D_{4d}) structure is the basic unit of the monoclinic (α, β, and γ) phases and has been studied often.[7,22,23] The measurements give bond lengths $d=2.34\pm0.006$ Å, bond angles $\alpha=105.7\pm1.6°$ and dihedral angles $\gamma=101.3°$. From Raman and infrared spectroscopy one deduces 11 vibrational modes with frequencies ranging from 1.41 to 7.68 THz,[24] and the gas phase binding energy is 2.24 eV/atom.[15] The MD/DF calculations give a structure with bond length 2.34 Å, bond angle 105°, dihedral angle 101°, and binding energy 3.28 eV/atom.

The ground state of Se_8 calculated with our model potential has $d=2.33$ Å, $\alpha=100°$, and $\gamma=101°$ and a binding energy of 2.24 eV, in good agreement with both experimental and MD/DF values. We find 11 vibrational modes with frequencies between 0.84 and 7.91 THz.

B. Crystals

The model potential is parametrized using the data for Se clusters, and refined using results for the trigonal and α-monoclinic phases. The quality of the potential is measured by its ability to describe quantities that are not used in the fitting procedure, and we now study some examples, including thermodynamic properties and structures of other crystalline phases.

Selenium possesses various crystalline modifications and undergoes numerous structural changes and phase transitions under pressure and/or heating.[25,26] The trigonal is the most stable of the six crystalline structures,[7] there are the two monoclinic phases (α and β forms) discussed above, and three cubic crystals have been investigated by Andrievski *et al.*[27] These authors found a simple cubic form of Se (one atom per unit cell) that transforms into an fcc structure on heating, and a third form with the diamond structure. Another monoclinic phase—the γ form—has been reported by Cherin and Unger.[23] Other stable crystals have orthorhombic and rhombohedral symmetry.[28]

We now examine further the trigonal and α-monoclinic phases. The former comprises infinite helical chains parallel to the c axis and is stable under normal conditions. In a chain the nearest-neighbor distance d_{NN} is 2.37 Å, the bond angle $\alpha=103.1°$, and the dihedral angle $\gamma=100.7°$. The helices have threefold periodicity, and the smallest separation between atoms in different chains (d_{NNN}) is 3.44 Å. The density of this phase is 4.81 g cm^{-3}.[29] The unit cell (with lattice constants $a=4.36$ Å and $c=4.95$ Å at room temperature) contains three atoms.

With our parametrized potential the trigonal state has lattice constants $a=4.45$ Å and $c=4.75$ Å, i.e., 2% higher and 4% lower than the experimental values, respectively. The intrachain parameters are $d_{\mathrm{NN}}=2.37$ Å, $\alpha=100.4°$, and $\gamma=98.6°$ for the nearest neighbor distance, the bond angle and the dihedral angle, respectively. The distance d_{NNN} is 3.45 Å, and the calculated density is less than 1% too high, so that the structure obtained with our potential agrees well with experimental findings.[8] The sublimation energy for a Se_8 molecule into the trigonal phase [$\Delta H_S(Se_8)=0.203$ eV/atom] is close to the experimental value (0.217 ± 0.013 eV/atom).[18]

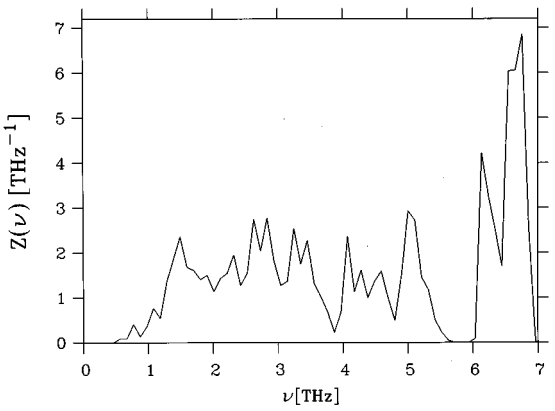

FIG. 4. Vibrational density of states Z as a function of frequency ν (THz) for a trigonal Se crystallite with 1470 atoms.

The dynamical and thermodynamic properties are very sensitive to the quality of a model potential. An approximate density of vibrational states can be derived from diagonalization of the dynamical matrix for a block with periodic boundary conditions. The elements are

$$D_{ij}^{\alpha\beta}=\frac{1}{\sqrt{M_i M_j}}\frac{\partial^2 U}{\partial R_i^{\alpha}\partial R_j^{\beta}}. \tag{5}$$

Here U is the total potential energy [Eq. (1)], the derivatives are with respect to the positions $\mathbf{R}_i$ and $\mathbf{R}_j$ of atoms i and j, and α and β stand for the Cartesian directions. M_i and M_j are the atomic masses. For a block containing N atoms one has to diagonalize a $3N\times 3N$ matrix, whose eigenvalues are the squares $[\omega_\sigma^2=(2\pi\nu_\sigma)^2]$ of the vibrational mode frequencies. Figure 4 shows the density of states $Z(\nu)$ calculated for a crystallite of 1470 Se atoms.

The spectrum can be divided roughly into three parts. The lowest frequency modes correspond to torsional vibrations and librations. Modes with frequencies in the range of 4–5 THz can be assigned to bond bending modes. One-third of all modes belongs to the high-frequency peak, which is separated by a gap of about 0.70 THz from the rest of the spectrum and is attributed to stretching vibrations. The experimental gap is larger, about 1.5 THz,[30] the high-frequency peak is too narrow and the maximum frequency too low, but otherwise our spectrum reproduces the experiment satisfactorily.

The small system size that can be treated in real space implies a minimum q value of the phonons calculated from Eq. (5). To calculate the long-wavelength phonons we, therefore, use the dynamical matrix in $\mathbf{q}$ space,[31]

$$D_{ij}^{\alpha\beta}(\mathbf{q})=\frac{1}{\sqrt{M_i M_j}}\sum_{kl}\frac{\partial^2 U}{\partial R_{ik}^{\alpha}\partial R_{jl}^{\beta}}\cdot e^{i\mathbf{q}(\mathbf{R}_{ik}-\mathbf{R}_{jl})}, \tag{6}$$

where α and β denote the Cartesian indices, k,l the unit cells, and i,j the sublattice, respectively. $\mathbf{R}_{ik}$ and $\mathbf{R}_{jl}$ are the atomic positions, and M_i and M_j the atomic masses. The summation is over all cells l,k within the interaction sphere. Diagonalization of the matrix $\mathbf{D}(\mathbf{q})$ yields as eigenvalues the squared phonon frequencies ω^2 and as eigenvectors the phonon polarization vectors. The trigonal phase of Se has three atoms per unit cell and therefore nine phonon branches.

In Fig. 5 we compare calculated and experimental[32] dispersion curves in the symmetry directions $[00\zeta]$, $[\zeta\zeta\frac{1}{2}]$, $[\frac{1}{3}\frac{1}{3}\zeta]$, $[\zeta\zeta 0]$, and $[\zeta 00]$, $[\zeta\zeta 0]$ in the usual reduced units. The differences between these curves reflect, of course, the inaccuracies of the potential model observed already in the spectrum. The high-frequency peak is too narrow and the dispersion of the high-frequency optic modes is too low. This effect has been reported earlier for Born–von Kármán type fits of the phonon dispersion.[33] The calculated lower branches, particularly the acoustic ones, are generally too hard. In some cases there is hybridization between optic and

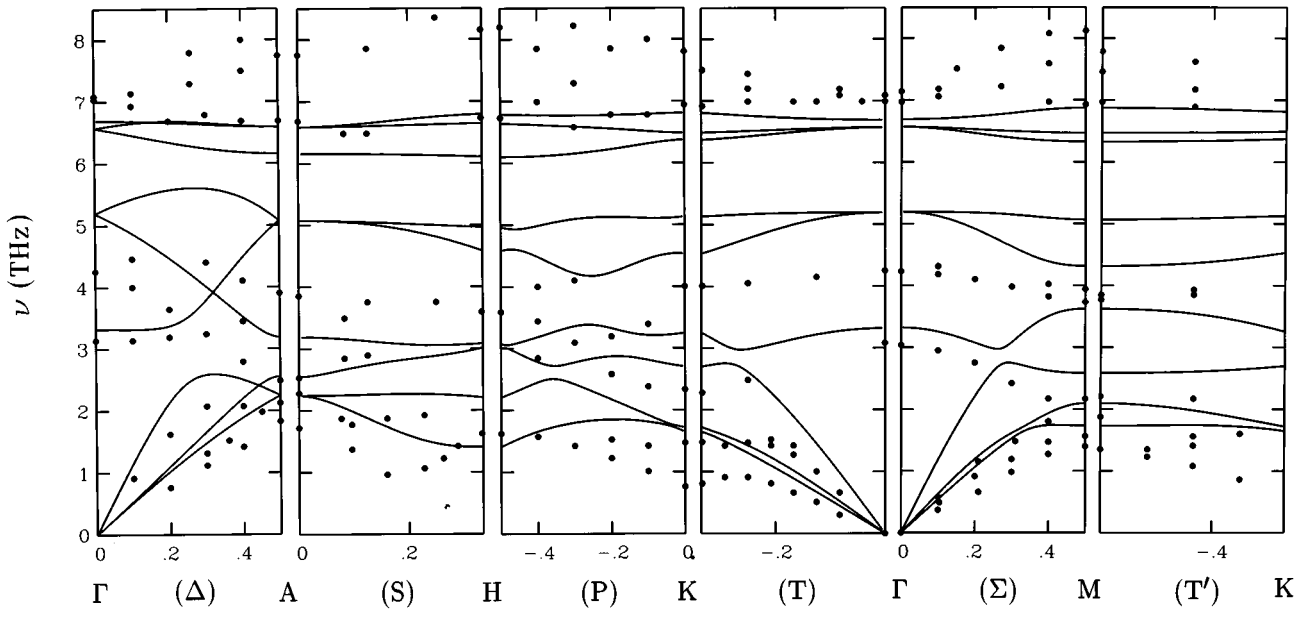

FIG. 5. Calculated (solid lines) and experimental (full circles, Ref. 32) phonon dispersion curves of trigonal Se plotted against reduced wave vector $\boldsymbol{\zeta}$.

acoustic branches that is not observed experimentally, but this leads only to slight shifts in the spectral density and weak effects in the dynamics in general. The lower branches can be made to agree with experiment if the range of the radial functions in the three-body potential [Eqs. (3) and (4)] is reduced by $\sim 10\%$. This would, however, impair the stability of the trigonal structure and hamper severely applications to defect or disordered structures.

The phonon frequencies have not been used in fitting the model potential, so that it is not surprising that the calculated phonon dispersion is less accurate than one obtained by a direct fit. However, the overall quality gives us confidence that the major dynamical effects will be reproduced correctly.

From the acoustic branches we derive some direction-dependent sound velocities. For the $[00\zeta]$ direction we have a longitudinal sound velocity $v_{33}=5630$ m s^{-1} at $T=0$ K, compared with 4350 m s^{-1} derived from the temperature dependence of the elastic constants.[34] The slope of the longitudinal acoustic branch in the $[\zeta 00]$ leads to the sound velocity $v_{11}=5330$ m s^{-1}, and hence $C_{1111}=C_{11}=142.0\times 10^9$ N m^{-2}. From the lowest transverse acoustic branch in the $[\zeta\zeta 0]$ direction we derive similarly $v_{66}=2400$ m s^{-1} and the elastic constant $C_{66}=28.8\times 10^9$ N m^{-2}. Meissner and Mimkes[34] have measured $C_{11}=25.0\times 10^9$ N m^{-2} with $v_{11}=2280$ m s^{-1}, and $C_{66}=10.0\times 10^9$ N m^{-2} with $v_{66}=1440$ m s^{-1}, respectively, at $T=0$ K.

The elastic constants and sound velocities can be obtained directly by compressing and straining the crystal. We apply a strain to the crystal by the transformation

$$R_i \rightarrow R_i + \sum_{j=1}^{3} \epsilon_{ij} R_j , \tag{7}$$

where $\mathbf{R}$ denotes the origin of the unit cell. If the lattice had been in equilibrium before applying the strain, the energy change is related to the elastic constants C_{ijkl} by

$$\Delta U = \frac{1}{2} \sum_{ijkl} \epsilon_{ij} C_{ijkl} \epsilon_{kl} . \tag{8}$$

We note that the relative positions of the three atoms in the unit cell generally change upon straining. The elastic constants calculated using the model potential are harder than those measured. By straining the crystal in the z direction, for example, we find $C_{33}=165.9\times 10^9$ N m^{-2}, while Meissner and Mimkes give a value extrapolated to $T=0$ K of $C_{33}=91.0\times 10^9$ N m^{-2}. This discrepancy reflects the fact that the calculated longitudinal sound velocity in the $[00\zeta]$ direction is higher than the experimental value.

The low-temperature properties of crystals are commonly characterized by a Debye temperature Θ_D. This is determined from a mean (Debye) sound velocity v_D, which can be calculated from the initial slopes of the three acoustic branches:

$$v_D = \left(\frac{1}{3} \sum_{i=1}^{3} \int \frac{1}{v_i^3} \frac{d\Omega}{4\pi} \right)^{-1/3} . \tag{9}$$

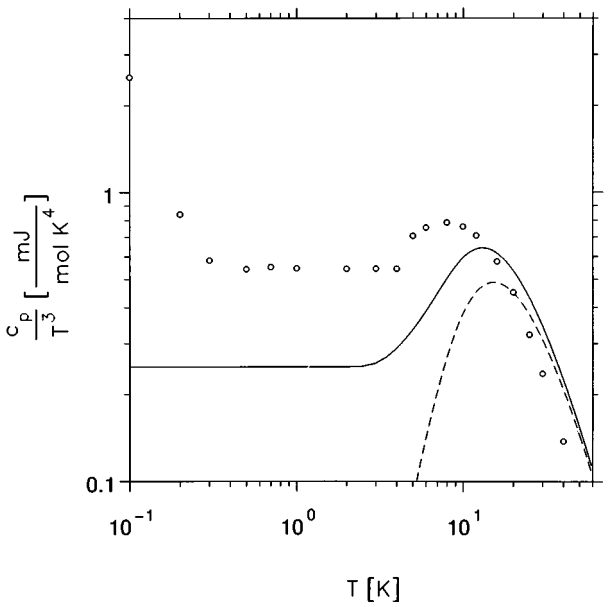

FIG. 6. Double-logarithmic plot of specific heat (c_p/T^3) of trigonal Se against temperature T (K), with (full line) and without (dashed line) Debye contribution. Open circles mark experimental values (Ref. 35).

The integration is over all directions and the summation is over the three acoustic branches. The Debye sound velocity in our model is $v_D=2588$ m s^{-1} (the experimental value is 1730 m s^{-1}),[29] from which we derive a Debye frequency ν_D of 5.2 THz and a Debye temperature Θ_D of 250 K (experimental values 3.8 THz and 181 K, respectively).[34]

From the vibrational density of states we calculate the specific heat c_p in the harmonic approximation:

$$c_p(T) = 3k_B \int d\omega \frac{(\hbar\omega/2k_BT)^2}{[\sinh(\hbar\omega/2k_BT)]^2} Z(\omega), \tag{10}$$

where $Z(\omega)$ is the vibrational density of states. The dashed line in Fig. 6 shows the temperature dependence of c_p/T^3, calculated from the spectrum Fig. 4. This spectrum does not include the long-wavelength acoustic modes ($q<q_{\min}$), so that we have added a Debye contribution cutoff at the frequency corresponding to $q_{\min}$ (full line). The strong peak at $T=14.9$ K shifts to 12 K after this correction, and is higher than in experiment (shown as open circles).[35] The low-temperature specific heat is too low, in accordance with the overestimates of the sound velocities and Debye temperature.

Besides the trigonal phase, consisting of infinite chains, one finds crystalline phases comprising Se_n molecules. The unit cells of the α-, β-, and γ-monoclinic phases consist of eight-membered rings with different packings. We now consider the first of these, which is the best studied of the three. Because the main feature of this structure—the Se_8 molecule—is described well with our model potential, the crystalline structure should also be reproduced well. In the α-monoclinic crystal (with four eight-membered rings) we find a bond length of 2.35 Å, bond angle 103.9°, and dihedral angle 101.5°, in good agreement with the experimental values (2.34 Å, 105.7°, and 101.3°, respectively).[7] The cal-

culated lattice constants are $a=8.64$ Å, $b=8.53$ Å, $c=11.58$ Å, and $\beta=86°$, compared with the corresponding experimental values 9.05 Å, 9.07 Å, 11.61 Å, and 90.46°.[8] The energy of this configuration lies 21.8 meV/atom above that of the trigonal phase, very close to the measured value (21.9 meV/atom).[35]

We have considered only twofold coordinated structures so far, and we now apply the potential to crystalline allotropes of Se with higher coordination numbers, including the cubic forms.[7] A striking feature of these structures is the variation in the coordination number for the diamond (4), simple cubic (6), and fcc structures (12). We have constructed crystals with diamond, sc, and fcc structures, respectively, and minimized the energies by relaxing the atomic positions and the volume using a steepest descents–conjugate gradient algorithm.[36] For the diamond structure, with a coordination number of four, the model potential gives a nearest-neighbor distance $d_{NN}=2.44$ Å under an external pressure $P_{ex}=3.5$ GPa, and d_{NN} becomes 2.47 Å in the absence of pressure. This structure has a unit cell with lattice constant $a=5.70$ Å and a density of 5.81 g cm^{-3}. Andrievski *et al.* found a diamond structure with eight atoms per unit cell (lattice constant $a=6.04$ Å), $d_{NN}=2.62$ Å, and a density of 4.76 g cm^{-3}.

The simple cubic form (with six nearest-neighbors) has $d_{NN}=3.05$ Å and a density of $\sim$4.68 g cm^{-3}, in reasonable agreement with measured values ($d_{NN}=2.97$ Å, density 5.00 g cm^{-3}).[27] For the fcc structure, calculations with the model potential give $d_{NN}=3.35$ Å, a lattice constant a of 4.71 Å, and a density of 5.11 g cm^{-1}, compared with experimental values of 4.07 Å, 5.76 Å, and 2.75 g cm^{-3}. We attribute the deviations to the neglect of the electronic degrees of freedom in the model.

IV. SUMMARY

We have developed a parametrized potential based on fitting the structures of small Se molecules, determined by density functional calculations[11] and experimental data, and refined to reproduce the structure of the trigonal crystal. The most important structural features of selenium are described with this interatomic potential, and the dynamics and thermodynamic properties are reproduced qualitatively. For the most stable crystalline structure the model potential yields values of the elastic constants that are too high and a Debye temperature that is too low. The relative stabilities of the different crystalline modifications are reproduced satisfactorily. Despite the explicit use of structures with twofold coordination for constructing the potential, it is remarkable that we can reproduce cubic structures with higher coordination numbers, as well as structural units and arrangements other than rings or chains.

The model potential does not treat the electronic degrees of freedom explicitly and cannot differentiate, for example, between different spin states of a system. To describe such features, or to make reliable predictions of unknown geometries, it is necessary to use parameter-free schemes such as MD/DF. The alternation of bond lengths common to sulfur and selenium is not reproduced by the model. However, the parametrization of forces and energies has the great advantage of allowing simulations to be performed in much larger systems and for much longer times than otherwise possible. The form of the potential we use allows bond breaking, which is not possible if one assumes a purely harmonic form, as in Born–von Kármán models. The potential can then be used in classical molecular dynamics (MD) simulations, which provide a convenient method for investigating the structural changes that occur, e.g., during the glass transition, and for the observation of (localized) relaxations in glasses,[12,13] which is outside the scope of simulations of small systems. We believe that it should be useful in other contexts.

ACKNOWLEDGMENTS

S.M.R. thanks the Studienstiftung des deutschen Volkes and the Forschungszentrum Jülich for support. The calculations were performed on the Cray Y/MP M94 computer of the Forschungszentrum Jülich.

*Present address: Institut für Algorithmen und Wissenschaftliches Rechnen, GMD-Forschungszentrum für Informationstechnik, D-53754 Sankt Augustin, Germany.

†Present address: The Niels Bohr Institute, University of Copenhagen, Universitetsparken 5, DK-2100 Copenhagen, Denmark.

[1] H. Bilz and W. Kress, *Phonon Dispersion Relations in Insulators* (Springer, Berlin Heidelberg, 1979).

[2] N.G. Almarza, E. Enciso, and F.J. Bermejo, Europhys. Lett. **17**, 595 (1992); M. García-Hernández, F.J. Bermejo, B. Fåk, J.L. Martinez, E. Enciso, N.G. Almarza, and A. Griado, Phys. Rev. B **48**, 149 (1993).

[3] For reviews, see R.O. Jones and O. Gunnarsson, Rev. Mod. Phys. **61**, 689 (1989); R.M. Dreizler and E.K.U. Gross, *Density Functional Theory* (Springer, Berlin Heidelberg, 1990).

[4] R. Car and M. Parrinello, Phys. Rev. Lett. **55**, 2471 (1985).

[5] D. Hohl and R.O. Jones, Phys. Rev. B **43**, 3856 (1991).

[6] C. Bichara, A. Pelegatti, and J.-P. Gaspard, Phys. Rev. B **49**, 6581 (1994).

[7] J. Donohue, *The Structures of the Elements* (Wiley, New York, 1974), p. 370.

[8] R.W.G. Wyckoff, *Crystal Structures* (Krieger, Malabar, FL, 1982), p. 36.

[9] A. Benamar, D. Rayane, P. Melinon, B. Tribollet, and M. Broyer, Z. Phys. D **19**, 237 (1991).

[10] J. Becker, K. Rademann, and F. Hensel, Z. Phys. D **19**, 229 (1991); **19**, 233 (1991).

[11] D. Hohl, R.O. Jones, R. Car, and M. Parrinello, Chem. Phys. Lett. **139**, 540 (1987); R.O. Jones (unpublished).

[12] C. Oligschleger and H.R. Schober, Physica A **201**, 391 (1993).

[13] C. Oligschleger and H.R. Schober, Solid. State Commun. **93**, 1031 (1995).

[14] F.H. Stillinger, T.A. Weber, and R.A. La Violette, J. Chem. Phys. **85**, 6460 (1986); F.H. Stillinger and T.A. Weber, J. Phys. Chem. **91**, 4899 (1987).

[15] K.C. Mills, *Thermodynamic Data for Inorganic Sulphides, Selenides and Tellurides* (Butterworths, London, 1974).

[16] Harwell Subroutine Library, routine VA05A.

[17] T.P. Martin, J. Chem. Phys. **81**, 4427 (1984).

[18] *Selected Values of the Thermodynamic Properties of the Elements*, edited by R. Hultgren, P.D. Desai, and D.T. Hawkins

(American Society for Metals, Metals Park, OH, 1973).
[19] K.P. Huber and G. Herzberg, *Molecular Spectra and Molecular Structure. Vol. IV. Constants of Diatomic Molecules* (Van Nostrand Reinhold, New York, 1979).
[20] V.E. Bondybey and J.H. English, J. Chem. Phys. **72**, 6479 (1980).
[21] H. Schnöckel, H.-J. Göcke, and R. Elsper, Z. Anorg. Allg. Chem. **494**, 78 (1982).
[22] R. Steudel and E.-M. Strauss, Adv. Inorg. Chem. Radiochem. **28**, 135 (1984).
[23] P. Cherin and P. Unger, Acta Crystallogr. B **28**, 31 (1972).
[24] R. Steudel and E.-M. Strauss, Z. Naturforsch. **36b**, 1085 (1981).
[25] T. Krüger and B. Holzapfel, Phys. Rev. Lett. **69**, 305 (1992); Y. Akakhama, M. Kobayashi, and H. Kawamura, Phys. Rev. B **47**, 20 (1993).
[26] K.E. Murphy, M.B. Altman, and B. Wunderlich, J. Appl. Phys. **48**, 4122 (1977).
[27] A.I. Andrievski, I.D. Nabitovich, and P.I Kripiakevich, Sov. Phys. Dokl. **4**, 16 (1959).
[28] Y. Miyamoto, Jpn. J. Appl. Phys. **19**, 1813 (1980).
[29] *Selen*, *Gmelin Handbuch der Anorganischen Chemie*, 8th ed., Ergänzungsband A3, edited by G. Czack, G. Kirschstein, and H.K. Kugler (Springer, Berlin Heidelberg, 1981).
[30] F. Gompf, J. Phys. Chem. Solids **42**, 539 (1981).
[31] M. Born and K. Huang, *Dynamical Theory of Crystal Lattices* (Clarendon, Oxford, 1958).
[32] W.D. Teuchert, R. Geick, G. Landwehr, H. Wendel, and W. Weber, J. Phys. C **8**, 3725 (1975).
[33] J. Etchepare, P. Kaplan, and M. Merian, in *Lattice Dynamics*, edited by M. Balkanski (Springer, Paris, 1978).
[34] M. Meissner and J. Mimkes, in *Physics of Selenium and Tellurium*, edited by E. Gerlach and P. Grosse (Springer, Berlin Heidelberg, 1979).
[35] U. Gaur, H.-C. Shu, A. Mehta, and B. Wunderlich, J. Chem. Phys. Ref. Data **10**, 89 (1981).
[36] R. Fletcher and C.M. Reeves, Comput. J. **7**, 149 (1964).